Int. J. Multiphase Flow Vol. 15, No. 4, pp. 605–626, 1989
Printed in Great Britain.

0301-9322/89 $3.00 + 0.00

AXIAL MASS FLOW DISTRIBUTION IN TWO LATERALLY INTERCONNECTED CHANNELS WITH BLOCKAGES

A. TEYSSEDOU,[1] A. TAPUCU,[1] M. GEÇKINLI[2] and M. MERILO[3]
[1]École Polytechnique, 2900 Eduard Montpetit, Montréal, Québec H3T 1J4, Canada
[2]Technical University of Istanbul, Ayazaga Kampusu, Maslak, Istanbul, Turkey
[3]Electric Power Research Institute, California, U.S.A.

(*Received* 12 *May* 1988; *in revised form* 3 *February* 1989)

Abstract—In this research the axial mass flow distribution of a two-phase flow in two laterally interconnected channels with plate or smooth blockages in one of them has been determined. The experiments were carried out with air–water mixtures at 20°C. The inlet mass fluxes were kept almost constant ($\simeq 2000$ kg/s m^2) and the inlet void fractions were set at different values in the two channels. Upstream from the blockage, the mass transfer from the blocked to the unblocked channel is very important and increases with increasing blockage severity. With unequal inlet void fractions a non-negligible fraction of liquid is transported from the high void to the low void channel before the onset of diversion cross-flow caused by the blockage. In the downstream region the mass exchanges between the channels are usually quite complex; still, mass flow equalization is reached before the end of the interconnected region.

Key Words: two-phase, subchannels, blockages, diversion cross-flow

1. INTRODUCTION

Most reactor fuel assemblies are arranged as rod-bundle fuel elements forming a network of interconnected subchannels through which the coolant circulates. Because of the multiple interactions between adjacent subchannels: *turbulent mixing*, *diversion cross-flow*, *void* and *buoyancy drift*, the thermal–hydraulic study of rod bundles is a complex task. A basic understanding of the above interactions under single- and two-phase flow conditions is essential to evaluating the behavior of the fuel channel under normal and off-normal operating conditions.

In this investigation the effect of blockages on subchannel flows has been studied. One of the consequences of the blockage of a subchannel or a group of subchannels is to divert, depending on the blockage severity, some or all of the flow into the neighboring unblocked subchannels. The flow recovery downstream of the blockage is a slow process and it may take many hydraulic diameters before the flow is restored to its far upstream value. Therefore, immediately downstream of the blockage, higher enthalpies will prevail in the blocked subchannels than in the unblocked ones, and the heat transfer in these regions may be impaired. Thus, an adequate prediction of the enthalpies and the heat transfer conditions in the downstream region requires detailed information on the flow redistribution caused by the blockage.

This paper presents data obtained on two-phase flow redistribution between two laterally interconnected channels when one of them is partially blocked.

2. PREVIOUS WORK

Single-phase Flows

The single-phase flow mixing between interconnected subchannels is governed by the following possible mechanisms: (i) turbulent mixing; (ii) secondary flows; (iii) molecular diffusion; and (iv) diversion cross-flow.

Stochastic pressure and flow fluctuations promote mixing by turbulent diffusion and this is known as "*turbulent mixing*". This mixing mechanism has been studied by Hetsroni *et al.* (1968), Skinner *et al.* (1969), Walton (1969), Galbraith & Knudsen (1971) and Kjellström (1972). Mixing

data obtained on interconnected subchannels is usually correlated as a function of the Stanton number and eddy diffusivity coefficients. However, turbulent diffusion models alone could not provide a satisfactory explanation of the experimental trends observed for different subchannel geometries.

Several authors (Hetsroni *et al.* 1968; Skinner *et al.* 1969; Kjellström 1972; Singh 1972; Rogers & Tahir 1975) argued the existence of secondary flows which may reach the gap region and enhance the turbulent mixing between subchannels. The first studies on secondary flows were carried out by Nikuradse (1926) and Prandtl (1926). Even though the velocities of secondary flows in interconnected channels are very low compared to the average axial velocities, they promote the energy and momentum transport to the gap region (Lyall 1971; Rogers & Tahir 1975; Trupp & Azad 1975).

For low Reynolds numbers and small gap clearances, a laminar sublayer around the gap may be formed which prevents the turbulent eddies from penetrating to the neighboring channel. Under these conditions, the major mixing mechanism consists of molecular diffusion (Galbraith & Knudsen 1971; Singh 1972).

Diversion cross-flow is the directed flow caused by radial pressure differences between adjacent subchannels brought about by the differences in the heat flux input and in the ratio of subchannel heat flow area to coolant flow area, and by the swelling or bowing of fuel rods which partially or totally block one or several subchannels. It is usual practice to model diverted flows by means of transverse pressure loss coefficients (Rogers & Todreas 1968; Khan *et al.* 1971; Weisman 1971; Tapucu 1977).

Diversion cross-flows induced by blockages under single-phase flow conditions have been fairly well studied (Steifel 1971; Rowe *et al.* 1973; Tapucu 1977; Creer *et al.* 1979; Gençay *et al.* 1984; Tapucu *et al.* 1984a, b). In general, it is observed that in the upstream region, the diversion cross-flow induced by blockages takes place over a relatively short distance. This distance depends on the blockage severity and increases with increasing severity. Downstream of the blockage, the recovery of the diverted flow by the blocked channel is a slow process and requires several tens of hydraulic diameters before the flow in this channel is restored to its original value. However, it has been observed (Creer *et al.* 1979; Gençay *et al.* 1984; Tapucu *et al.* 1984a, b) that the pressure differences between the channels approach zero quite rapidly in this region.

Two-phase Flow

Under two-phase flow conditions there exist two additional mixing mechanisms which may act simultaneously with those observed for single-phase flows: "*void drift*" and "*buoyancy drift*". However, because of the highly stochastic nature of two-phase flows only the following four mixing phenomena are considered as the most relevant (Tahir & Carver 1984): (i) turbulent mixing; (ii) void drift; (iii) buoyancy drift; and (iv) diversion cross-flow.

The sophisticated instrumentation necessary to measure two-phase flows has often limited the experiments to air–water mixtures and to relatively simple subchannel geometries (Rousel & Beghin 1966; Walton 1969; Bestenbreur & Spigt 1970; Van der Ros 1970; Gonzalez-Santalo 1971; Singh 1972; Rudzinski *et al.* 1972; Shoukri *et al.* 1982; Tapucu *et al.* 1986). However, experiments have also been conducted with boiling fluorocarbons by Bowring & Levy (1969), Petrunik (1973) and others. Using sophisticated experimental setups, Rowe & Angle (1969), Lahey *et al.* (1971) and Castellana & Casterline (1972) have collected boiling water mixing data.

In single-phase flows, in the absence of mixing mechanisms others than turbulence, the subchannel flow remains essentially constant, as does the pressure level in each subchannel at any axial position. Therefore, in this flow there is little or no net mass transfer. In two-phase flows, in addition to momentum and energy transfer there will likely be a substantial net mass transfer induced by turbulence. Van der Ros (1970) modeled the turbulent gas mass exchanges as a diffusion process with the transverse void gradient as the driving force. However, it is a well-known fact that the void distribution may tend toward a nonuniform equilibrium void distribution and non-negligible void gradients may exist between the subchannels when the net gas mass transfer is zero. This behavior is explained by the "*void drift*" mechanism, observed for both adiabatic and diabatic flow conditions (Lahey & Schraub 1969; Lahey *et al.* 1972). Lahey *et al.* (1972) and Gonzalez-Santalo (1971) attempted to model the void drift on the basis of a diffusion process.

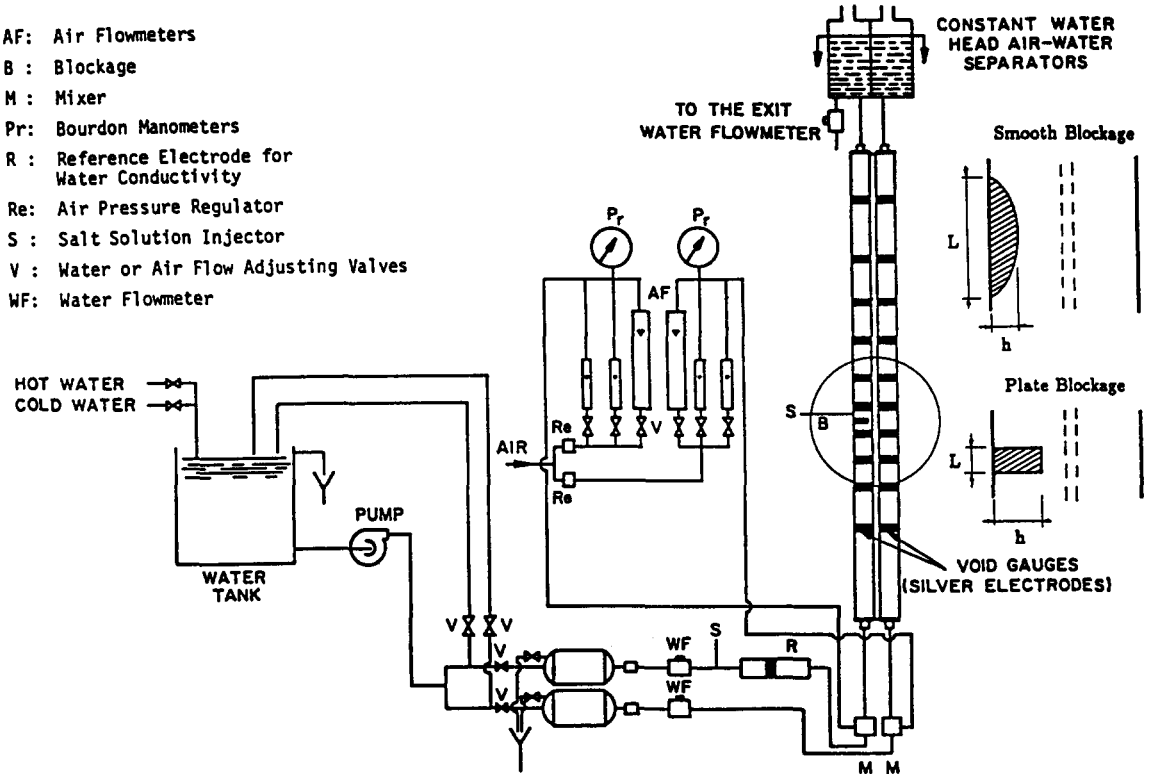

Figure 1. Experimental facility.

In horizontal subchannels, the void is pushed upward normal to the major flow direction due to the difference in densities between the phases. This phenomenon, known as "*buoyancy drift*", may force the flow toward a stratification. Shoukri *et al.* (1982) carried out horizontal two-phase flow experiments to determine turbulent mixing and gravity separation effects. Diversion cross-flows associated with unequal inlet flow conditions to the subchannels have been studied for vertical and horizontal two-phase flows by Tapucu and coworkers (Tapucu *et al.* 1986; Tapucu & Gençay 1980).

3. EXPERIMENTAL FACILITY

Figure 1 shows the experimental facility used to perform the blockage experiments. The test section (figure 2) is made up of two 12.65 mm square channels machined from transparent acrylic blocks. The channels are separated by an intermediate plate in which a slot was machined. The

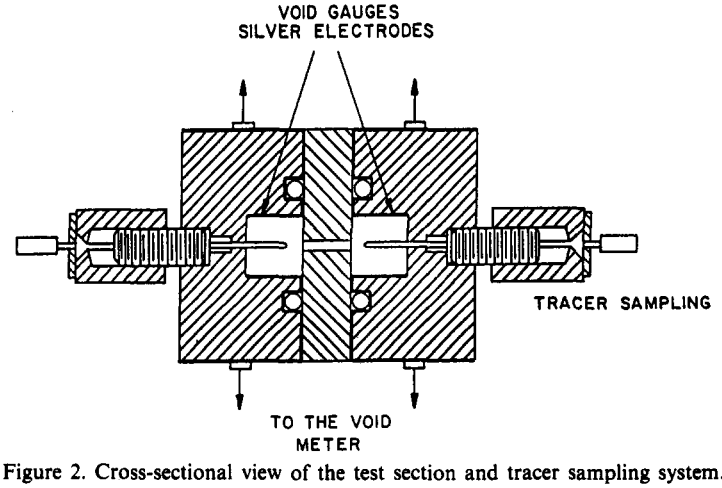

Figure 2. Cross-sectional view of the test section and tracer sampling system.

Table 1. Geometric parameters of the test section

Gap clearance	1.5 mm
Gap thickness	3.2 mm
Hydraulic diameters	
Channel 1[a]	12.7 mm
Channel 1	12.4 mm
Channel 2[a]	12.8 mm
Channel 2	12.6 mm
Cross-sectional area	
Channel 1	160 mm^2
Channel 1[a]	162.4 mm^2
Channel 2	163.1 mm^2
Channel 2[a]	165.5 mm^2
Length of the interconnection	1312 mm

[a]Including half of the interconnecting gap.
The mid-plane of the blockage is located 272 mm downstream of the interconnection.

relevant geometric parameters of the test section are given in table 1. Plate and smooth blockages (figure 1) of varying severities were mounted in channel 1 on the wall opposite to the interconnection gap, approx. 22 hydraulic diameters (D_h) downstream of the beginning of the interconnected region.

The water is supplied to the channels with a pump connected to a constant head water tank. The air is supplied from the mains of the laboratory and regulated by a relieving-type regulator. The mixing of the liquid and the gas phases is accomplished in a mixer. The average diameter of the generated bubbles, determined by a photographic method, was found to be of 1.5 mm. At the outlet of the test section, the two-phase mixture flows into an air–water separator tank which consists of two compartments, one for each channel. The compartments are open to the atmosphere and their water levels are kept constant. The water flow rates at the inlet of each channel and at the outlet of channel 1 after the separator tank are measured with turbine flowmeters. The flow rate of the air is measured with rotameters.

The measurement of liquid-phase mass exchanges between the blocked and unblocked channels is achieved by injecting a NaCl solution into the blocked channel and determining the variation of NaCl concentration in both channels by sampling the liquid phase. A schematic of the tracer sampling system is given in figure 2. For sampling in the region upstream of the blockage, the NaCl solution was injected before the phase mixer; for sampling in the downstream region, the injection was done in the recirculation zone which develops behind the blockage. The turbulence prevailing in this zone ensures an adequate mixing of the brine with the flow over a very short distance. A $KMnO_4$ dye solution was injected in this region to verify this feature. The sampling is performed at three locations in the region upstream of the blockage and at seven locations in the downstream region. To get a good idea of the average concentration at a given location, the sampling is also done at five equidistant points in the transverse direction. Additional sampling was also performed at the inlet of the blocked channel when the tracer was injected before the mixer and at the exit of both channels when it was injected immediately downstream of the blockage. The NaCl concentration in the samples was determined by a conductivity meter with an accuracy of $\pm 1\%$. The average tracer concentration was 600 mg/l and it is assumed that the physical properties of water, except its conductivity, are not affected.

Two blockage configurations have been studied: plate and smooth. The shape of the latter was a cosine. The plate blockage could be moved continuously in the transverse direction to achieve any blockage fraction. Table 2 gives the geometric parameters of the blockages.

4. EXPERIMENTAL PROCEDURES

Liquid-phase Mass Exchanges

In section 3 we outlined the method with which the liquid mass exchange between the channels were determined. The NaCl concentrations in both channels in conjuction with the tracer mass conservation equation allow the determination of the liquid masses exchanged between the channels. Figure 3 shows the liquid mass flow entering and leaving the control volumes as well as

Table 2.

Plate Blockage			
Area reduction (%)[a]	31.9	61.0	90.0
Thickness, L (mm)	3.2	3.2	3.2
Height, h (mm)	4.1	7.9	11.6
Smooth Blockage			
Area reduction (%)[a]	58.0		88.1
Length, L (mm)	49.9		50.5
Height, h (mm)	7.5		11.4

[a]Including half of the interconnecting gap.

the tracer influx and efflux. Applying the tracer mass conservation principle to the control volumes, yields:

blocked channel (i),

$$C_i\delta w - C_j\delta w' = -\frac{\partial(C_i m_i)}{\partial z}\,\mathrm{d}z; \qquad [1]$$

and

unblocked channel (i),

$$C_i\delta w - C_j\delta w' = \frac{\partial(C_j m_j)}{\partial z}\,\mathrm{d}z; \qquad [2]$$

where δw and $\delta w'$ are the mass exchanges between the channels, and m and C are the mass flow rate and the average tracer concentration in the channels, respectively. Discretization of these equations yields the following relationships.

Blocked channel (i)

(a) Tracer injection upstream from the blockage,

$$m_{i,n+1} = m_{i,n}\frac{C_{i,n} - C_{j,n+1}}{C_{i,n+1} - C_{j,n+1}} - m_{j,n}\frac{C_{jn+1} - C_{j,n}}{C_{i,n+1} - C_{j,n+1}}. \qquad [3]$$

(b) Tracer injection downstream from the blockage,

$$m_{i,n} = m_{i,n+1}\frac{C_{i,n+1} - C_{j,n}}{C_{i,n} - C_{j,n}} + m_{j,n+1}\frac{C_{j,n+1} - C_{j,n}}{C_{i,n} - C_{j,n}}. \qquad [4]$$

Exchanging the subindices i and j, two similar equations for the unblocked channel may be obtained. In order to use these equations the inlet concentrations $C_{i,0}$ and $C_{j,0}$, the outlet concentrations $C_{i,N}$ and $C_{j,N}$, the inlet flow rates $m_{i,0}$ and $m_{j,0}$, and the outlet flow rate in the blocked channel $m_{i,N}$ have to be measured.

The uncertainties in the liquid mass transfer are $\pm 3\%$; however, close to the blockage these uncertainties are expected to be about $\pm 12\%$.

Net Gas Mass Transfer

The net gas mass transfer from the blocked channel to the unblocked channel in the upstream region of the blockage, and in the opposite direction in the downstream region is determined by three different methods. They employ, respectively:

1. The relationship between the volumetric flow quality, the void fraction and the mass flow rate of the liquid phase ($\langle\beta\rangle = \beta(\epsilon, m_L)$).
2. The relationship between the averaged volumetric flux of the gas, the void fraction and the mass flow rate of the liquid phase ($\langle J_G\rangle = J_G(\epsilon, m_L)$).
3. The relationship between the void fluctuations propagation velocity, the void fraction and the mass flow rate of the liquid phase ($U = U(\epsilon, m_L)$).

The above relationships have been determined by Tapucu *et al.* (1988) using a single channel without blockage. Their application to interconnected channels is justified by the fact that the

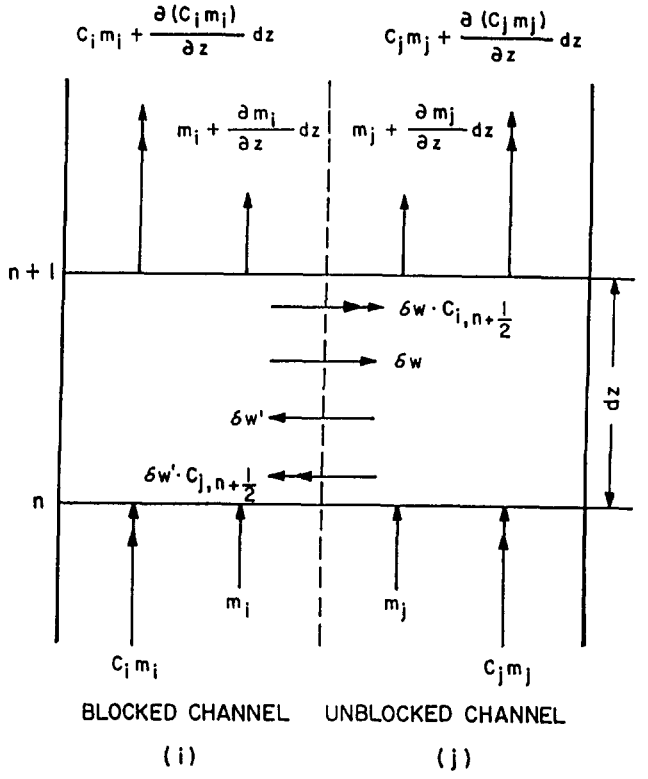

Figure 3. Control volume for liquid mass exchange.

responses of the conductive void gauges, under vertical flow conditions, are quite insensitive to the radial void distributions. In turn, the absolute pressure of the flow measured at the middle of the test section during single-channel experiments differs from those of two interconnected channels; therefore, the dependence of each of these relationships on the absolute pressure has also been studied. It has been observed that only the $\langle J_G \rangle$ function required a pressure correction.

1. Method based on the volumetric flow quality $\beta(\epsilon, m_L)$

This method consists of using the information on liquid mass flow rates (as determined by the tracer technique) and void fractions along the interconnected region (Tapucu *et al.* 1988) in conjunction with the volumetric flow quality curve given in figure 4. The volumetric flow quality is defined by

$$\langle \beta \rangle = \frac{Q_G}{Q_G + Q_L}, \qquad [5]$$

where Q_G and Q_L are the volume flow rates of the gas and liquid phases. From this equation Q_G can be written as

$$Q_G = Q_L \frac{\langle \beta \rangle}{1 - \langle \beta \rangle}. \qquad [6]$$

In this equation the void fraction and liquid mass flow rates are known and the values of β in the blocked and unblocked channel are determined from figure 4. An error analysis showed that the uncertainty in this method depends on the void fraction and for void fractions varying from 10 to 60% the uncertainties are between ± 6 and $\pm 12\%$. Therefore, for better accuracy, the gas mass flow rates were determined in the low void channel. The gas mass flow rates in the high void channel were then obtained from mass balance considerations.

2. Method based on the volumetric flux of the gas $J_G(\epsilon, m_L)$

In this method, the volumetric flux of the gas, $J_G(\epsilon, m_L)$ (figure 5), was used instead of the volumetric flow quality to determine the gas flow rates. Because of the pressure difference which

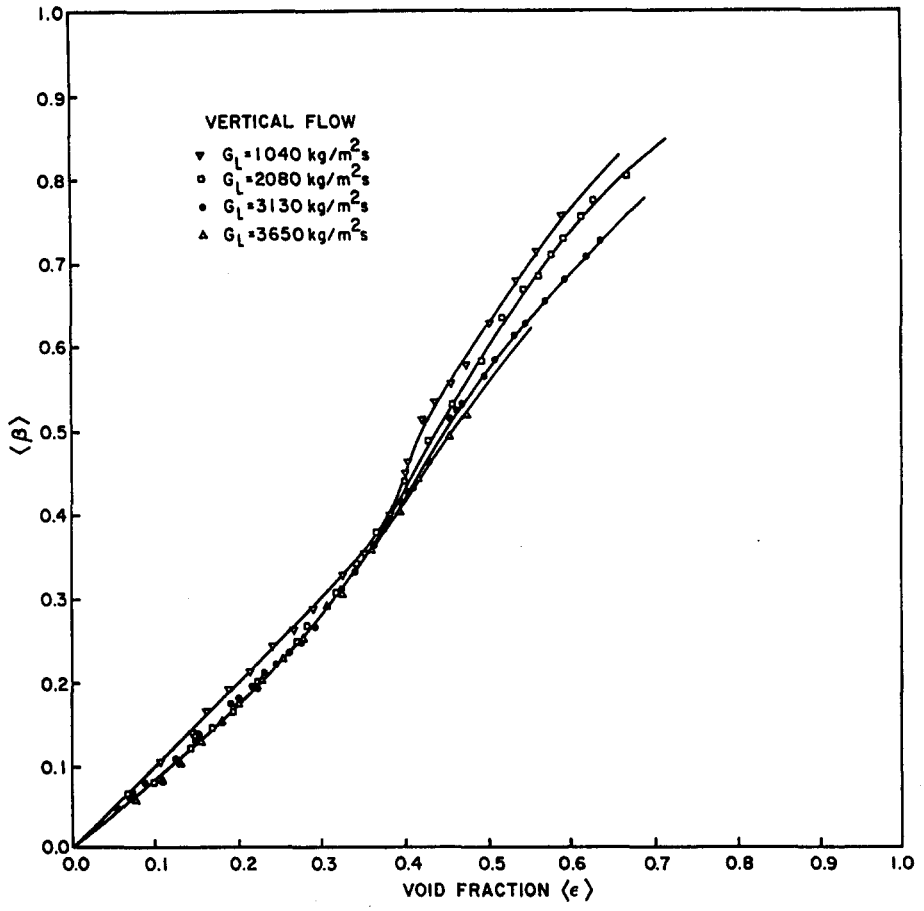

Figure 4. Relationship between volumetric flow quality and void fraction.

exists between the single-channel and two-channel blockage experiments, the value of $\langle J_G \rangle$ for a given void fraction and liquid mass flow rate in the interconnected region should be corrected. This correction is done by using empirical relationships previously determined under single-channel flow conditions.

The mixture mass conservation equation for steady-state two-phase flows is given by

$$\frac{\partial}{\partial z}(\langle J_L \rangle \rho_L + \langle J_G \rangle \rho_G) = 0. \quad [7]$$

Assuming an adiabatic flow, the above equation yields:

$$\frac{\partial}{\partial z}\langle J \rangle = -\langle J_G \rangle \frac{1}{p}\frac{\partial p}{\partial z}. \quad [8]$$

For two interconnected channels, the discretized form of this equation is written as

$$J^1_{Gi+1} + J^2_{Gi+1} = \left(1 - \frac{p^1_{i+1} - p^1_i}{p^1_{i+1/2}}\right) J^1_{Gi} + \left(1 + \frac{p^2_{i+1} - p^2_i}{p^2_{i+1/2}}\right) J^2_{Gi}. \quad [9]$$

This equation is used to calculate the gas mass flow rates in the blocked or unblocked channel. The inlet volumetric fluxes are known and the values of J^1_{Gi+1} (or J^2_{Gi+1}) are taken from figure 5. For the above void fraction range the uncertainties of this method vary from ± 4 to $\pm 12\%$.

3. Method based on the void fluctuation propagation velocity

In this method, the information on the $U/\langle J_G \rangle$ ratio obtained under single-channel flow conditions (figure 6) has been employed to determine the gas flow rates. In two interconnected channels, the variation of the void fluctuation propagation velocity has been determined by

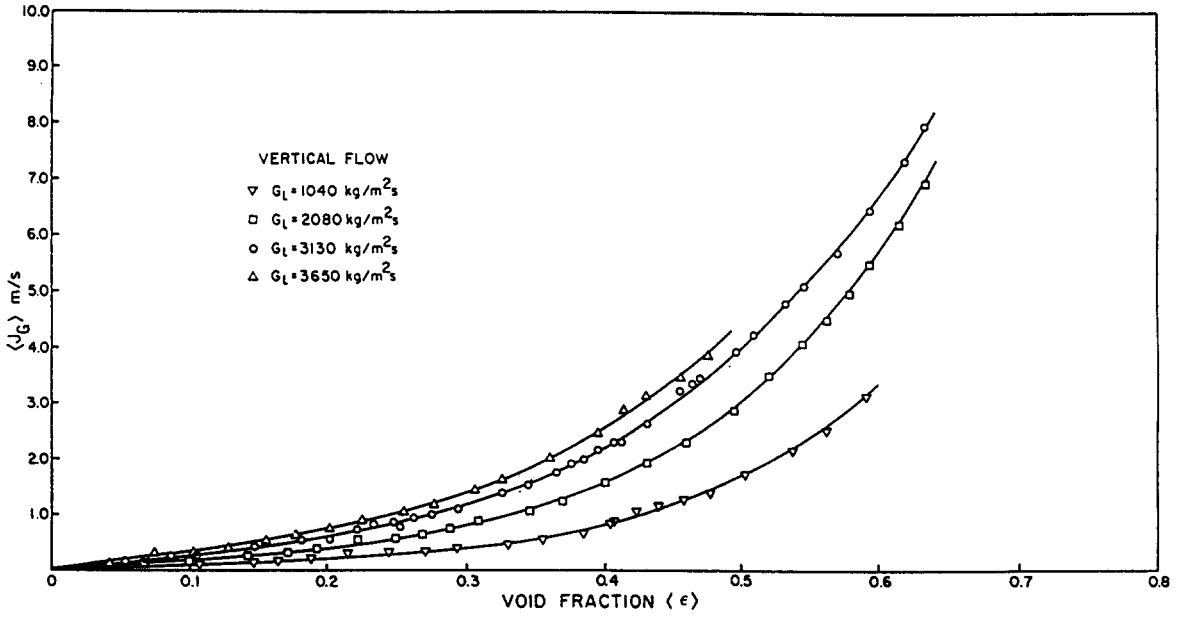

Figure 5. Relationship between volumetric flux of the gas and void fraction.

cross-correlating the void signals produced by two successive void gauges. This information in conjunction with the void fractions and liquid mass flow rates in the channel and the relationship $[U/\langle J_G\rangle]_{cal}$ shown in figure 6, enable us to calculate the gas mass flow rate with

$$\langle J_G\rangle_{tch} = U_{tch}\left[\frac{U}{\langle J_G\rangle}\right]_{cal}. \qquad [10]$$

$[U/\langle J_G\rangle]_{cal}$ is obtained by using the void fractions and the liquid mass flow rates as measured in two interconnected channels. The basic assumption made in this method is that, for a given void fraction, the void fluctuation propagation velocity is insensitive to the void profile differences which may exist between the single-channel flow and two-interconnected-channel flow because of the lateral inflow and outflow. This assumption does not hold true when lateral inflow and outflow are substantial, i.e. in the neighborhood of the blockage. Therefore, the results of this method should only be accurate for regions far from the blockage. For the above void fraction range the uncertainties of this method vary from ± 4 to $\pm 9\%$. However, close to the blockage this method is not reliable.

5. EXPERIMENTAL RESULTS

Three blockage fractions have been used for plate blockages—30, 60 and 90%; whereas smooth blockages were limited to blockage fractions of 58 and 90%. For each blockage fraction a set of three experiments was conducted:

1. Equal void fractions at the inlet of each channel.
2. Unequal inlet void fractions with high void at the inlet of the blocked channel.
3. Unequal inlet void fractions with high void at the inlet of the unblocked channel.

The inlet mass flux in each channel was maintained almost constant for all the runs ($\simeq 2000$ kg/s m^2).

Following the groups identified above, this paper presents the axial mass flow distributions obtained for 30 and 90% plate blockages, and for a 58% smooth blockage. More data on liquid and gas flow rates are given by Tapucu *et al.* (1988).

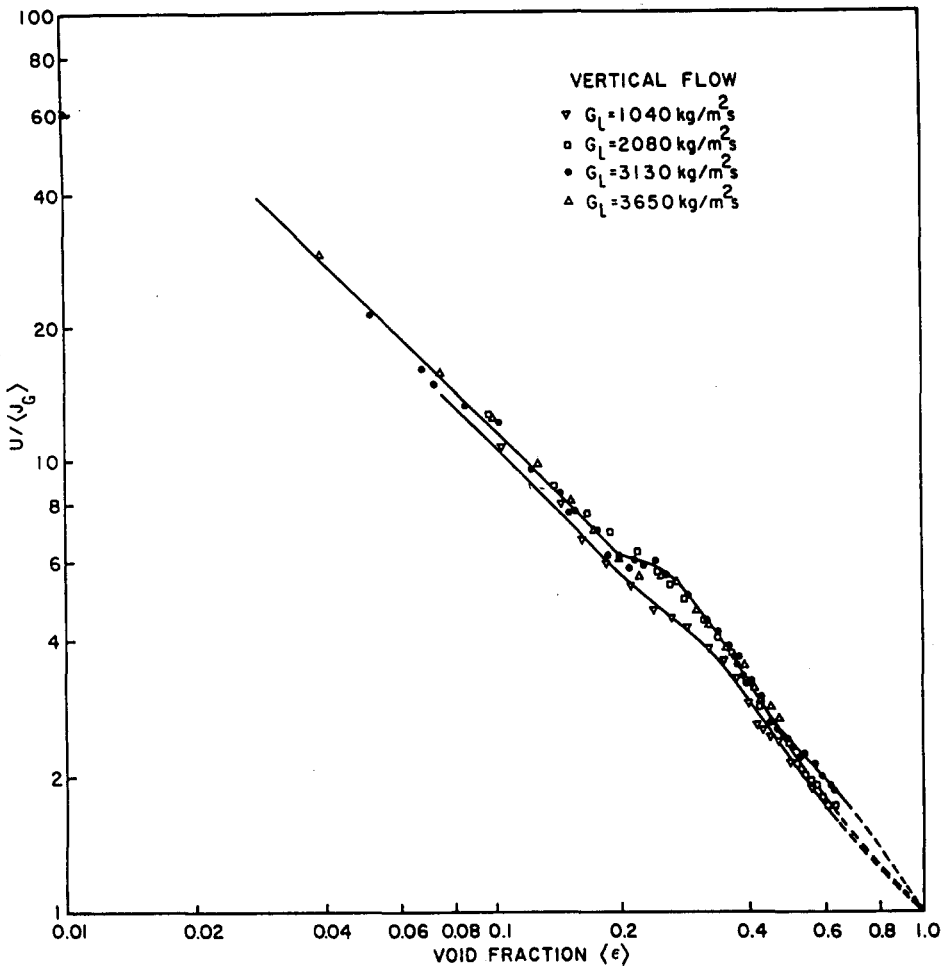

Figure 6. Variation of $U/\langle J_G \rangle$ with void fraction.

Liquid Mass Flow Rates

1. Equal void fraction at the inlet of the blocked and unblocked channels

In the upstream region the effect of the 30% plate blockage and 58% smooth blockage on the liquid transfer is felt approx. 190 mm from the blockage (figures 7.1a and 7.2a). For 90% plate blockage practically all the liquid is transferred from the blocked channel to the unblocked channel (figure 7.3a).

In the downstream region, the mass exchanges between the channels are quite complex. For 30% plate and 58% smooth blockages, the blocked channel first recovers more liquid than it lost (figures 7.1a and 7.2a). Consequently, the flow rate in this channel exhibits a maximum and then decreases. For 90% plate blockage the liquid recovery is a relatively fast process (figure 7.3a). A tendency toward an equalization of the liquid flow rates in the channels is observed far from the blockage (45 D_h for 30% plate and 58% smooth blockages and 20 D_h for 90% plate blockage).

2. Unequal void fractions with high void at the inlet of the blocked channel

In the upstream region, the mass flow rates in the blocked channel start decreasing with the beginning of the interconnection (figures 7.4a, 7.5a and 7.6a). Far from the blockage this decrease is mainly due to the net liquid transfer from the high void channel to the low void channel. Figure 7.10a, reproduced from Tapucu & Gençay (1980) shows the liquid mass flow rates in two laterally interconnected channels without blockage. It is observed that immediately after the beginning of the interconnection the liquid flow rates in the low void channel increase quickly to an asymptotic value. The net liquid transfer is mainly due to the diversion cross-flow induced by

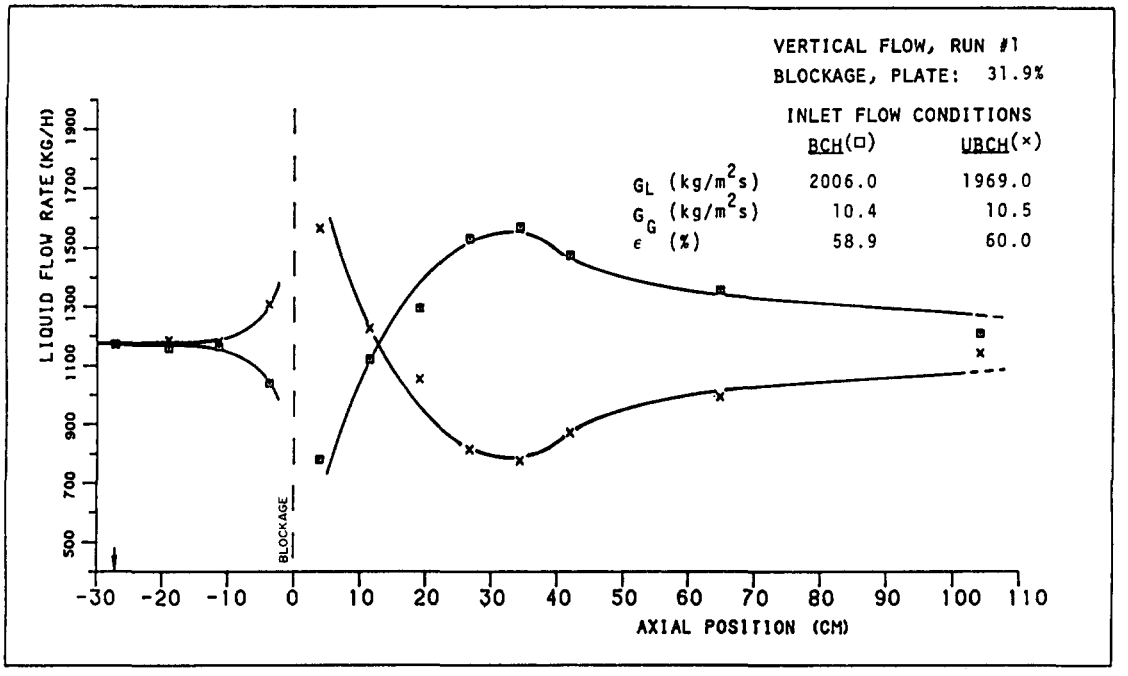

Figure 7.1a. Liquid mass flow rates in the blocked (BCH) and unblocked (UBCH) channels.

the pressure difference between the channels and also to the liquid carried by the bubbles during their migration from the high void channel to the low void channel. The same behavior is also observed in blocked interconnected channels far upstream of the blockage. The effect of the blockage is felt as far as 120 mm (10 D_h) in the upstream region.

In the downstream region, for 30 and 90% plate blockages (figures 7.4a and 7.6a), the blocked channel gradually recovers the liquid it lost. In this region, for 58% smooth blockage, figure 7.5a, the blocked channel recovers more liquid than it lost, goes through a maximum and then decreases to reach an asymptotic value. Far from the blockage the differences between the flow rates in the channels are not substantial.

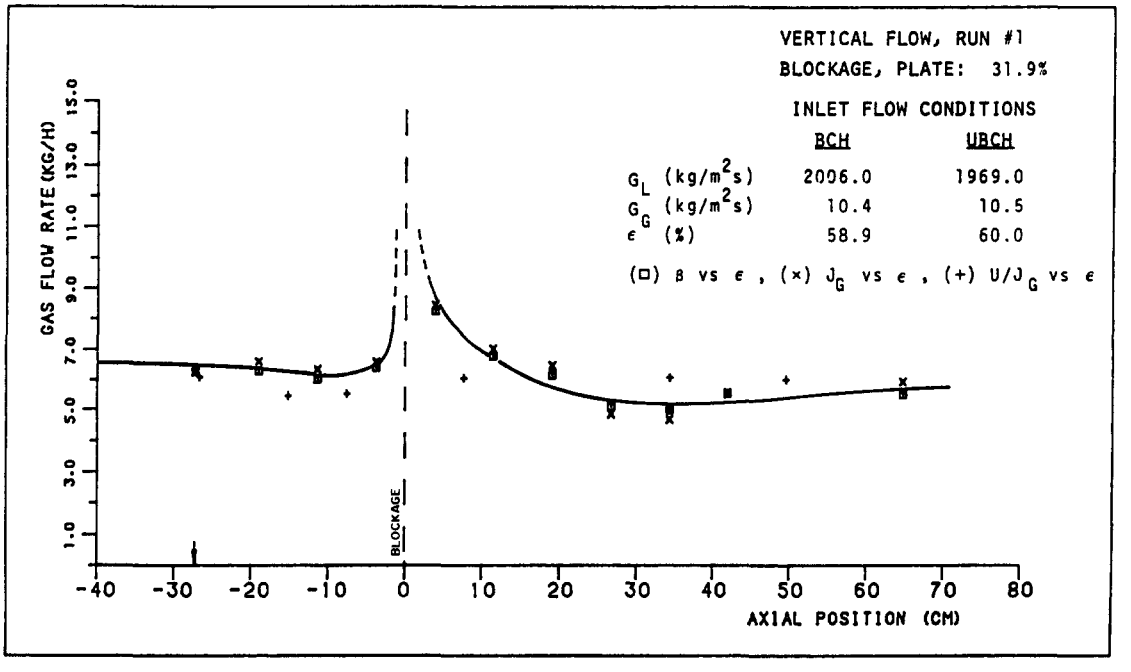

Figure 7.1b. Gas mass flow rates in the unblocked channel.

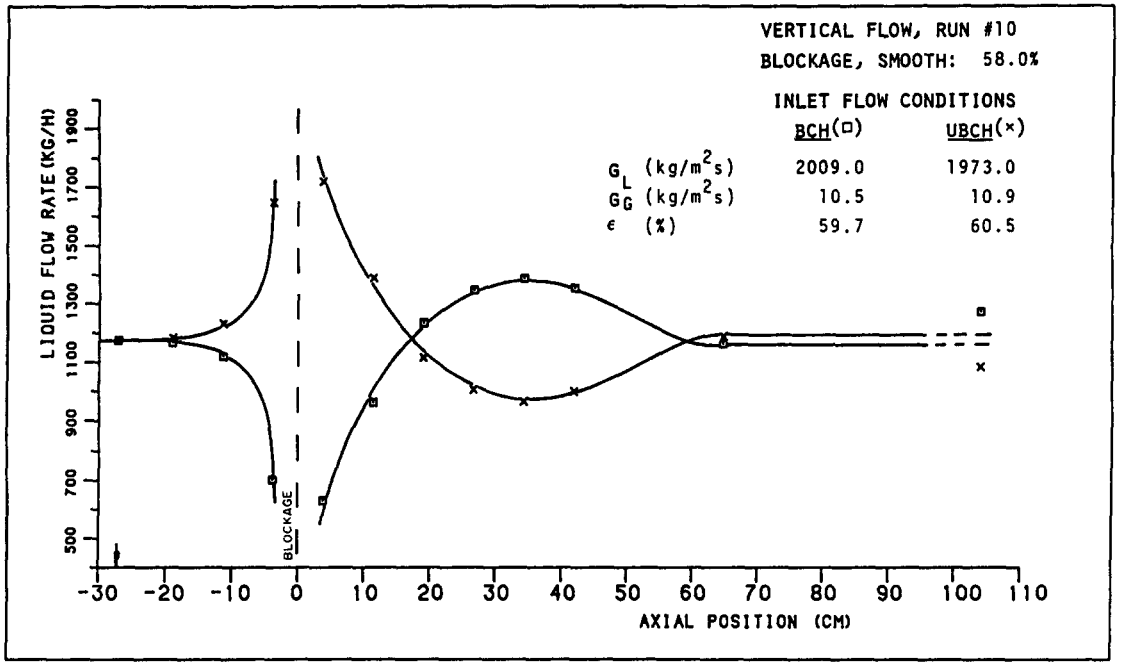

Figure 7.2a. Liquid mass flow rates in the blocked (BCH) and unblocked (UBCH) channels.

3. Unequal void fractions conditions with high void at the inlet of the unblocked channel

Upstream of the blockage, for 30% plate blockage (figure 7.7a) and 58% smooth blockage (figure 7.8a), the liquid flow rate in the blocked channel first increases slightly and then starts decreasing. The liquid transfer caused by the void difference between the channels and that caused by the presence of the blockage act in opposite directions and depending on the relative importance of each of these components the flow rate in the blocked channel increases or decreases. Far upstream of the blockage, the blocked channel receives more liquid than it has lost; therefore, the flow rates increase. The situation reverses close to the blockage where a decrease in the flow rate is observed. For 90% plate blockage (figure 7.9a) the diversion cross-flow caused by the blockage

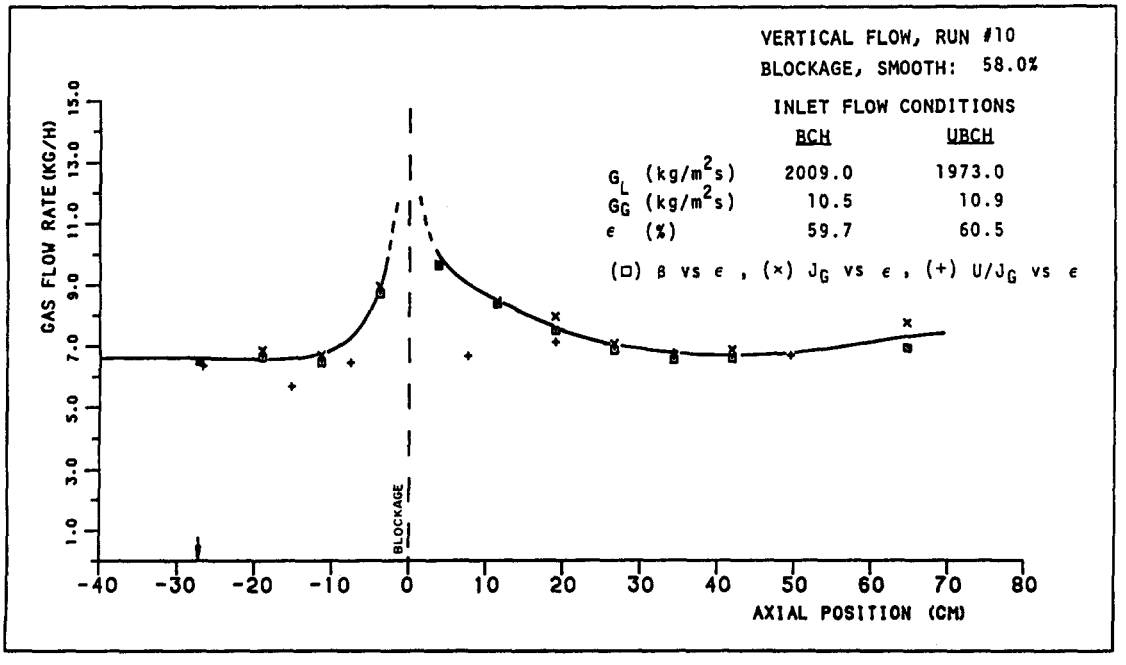

Figure 7.2b. Gas mass flow rates in the unblocked channel.

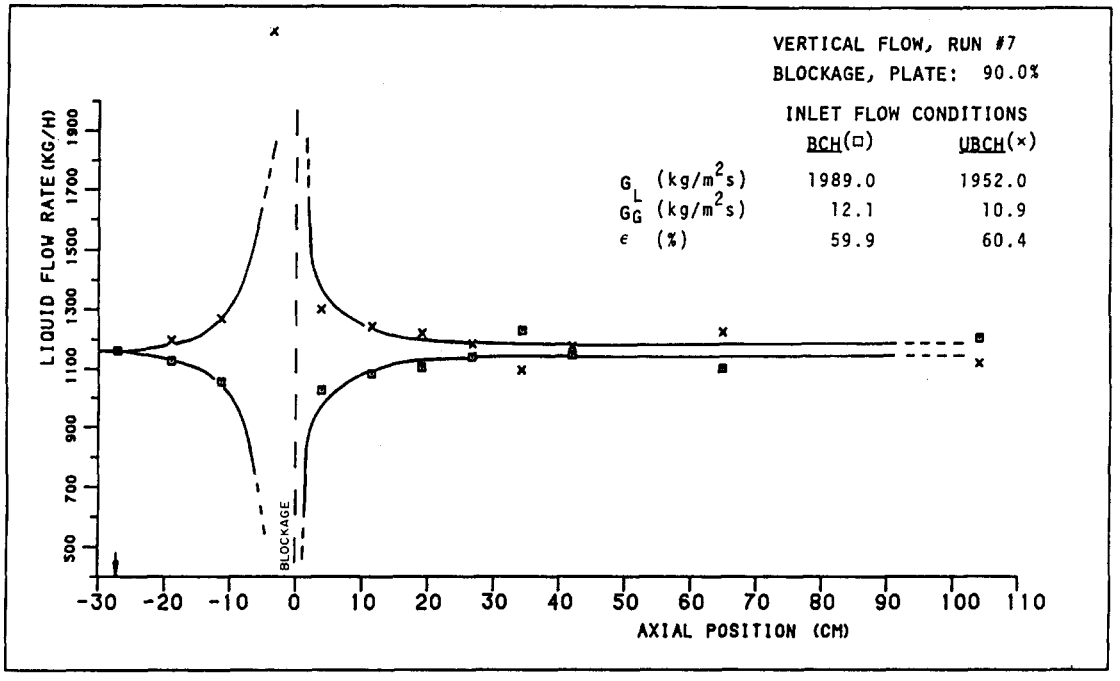

Figure 7.3a. Liquid mass flow rates in the blocked (BCH) and unblocked (UBCH) channels.

is overwhelming; therefore, flow rates in the blocked channel decrease slowly at first and then very quickly close to the blockage.

The flow rate downstream of the 30% plate blockage (figure 7.7a) increases very rapidly past its original value and then decreases to establish almost equal flow rates in the channels. The same pattern is also observed for the 58% smooth blockage (figure 7.8a) with the only difference being the flow rate in the blocked channel decreases slightly after reaching its original value. For the 90% plate blockage (figure 7.9a) the flow recovery by the blocked channel is quite slow and long distances are required to achieve equal flow rates in the channels.

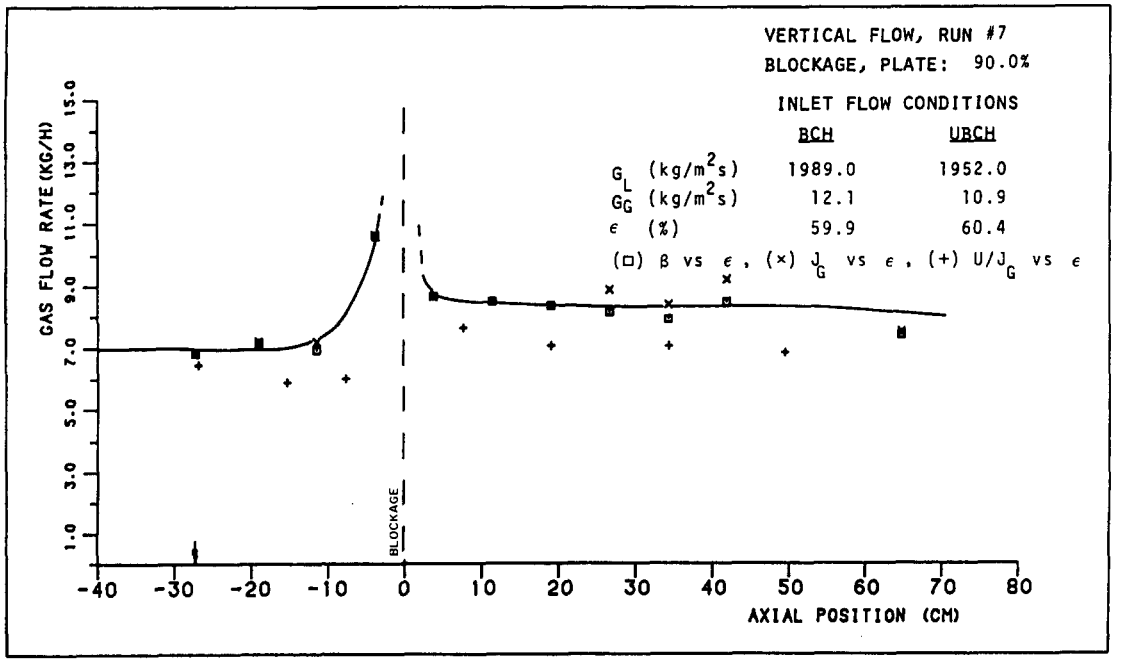

Figure 7.3b. Gas mass flow rates in the unblocked channel.

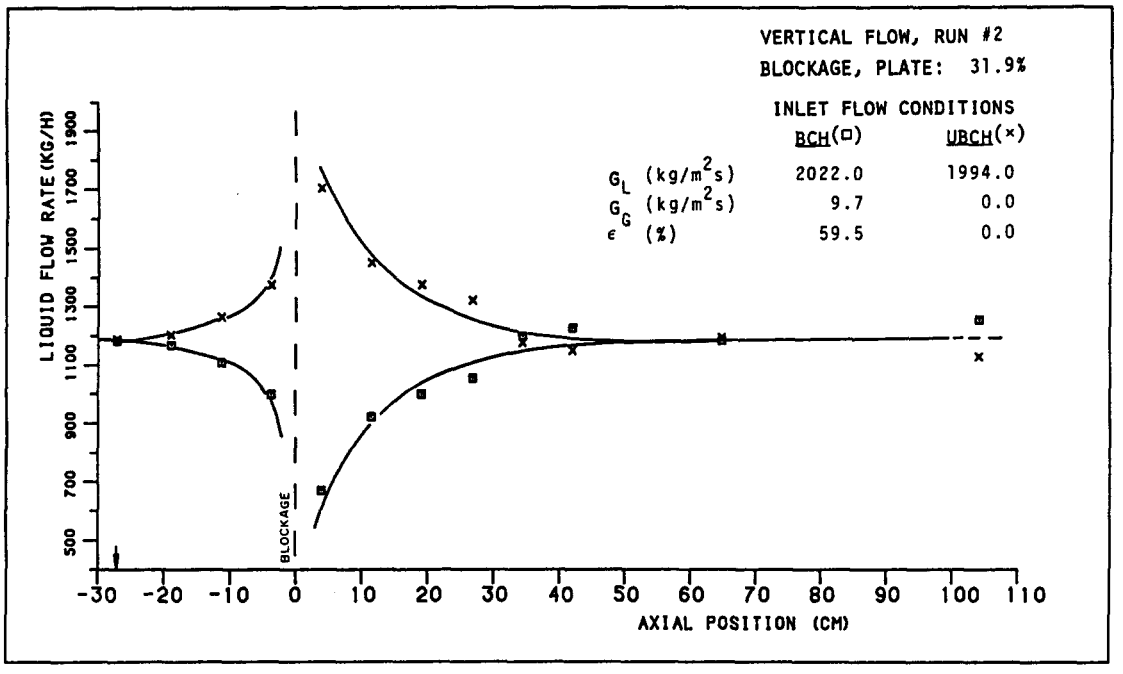

Figure 7.4a. Liquid mass flow rates in the blocked (BCH) and unblocked (UBCH) channels.

Gas Mass Flow Rates

The net gas mass transfer from the blocked channel to the unblocked channel in the upstream region of the blockage, and in the opposite direction in the downstream region was determined by the three different methods outlined in section 4. These methods were based on the volumetric flow quality, the volumetric flux of the gas and the void fluctuations propagation velocity. Figures 7.1b–7.9b show the gas mass flow rates obtained in the unblocked channel by the above three methods. The agreement between the first and the second methods is always excellent. The agreement of the third method with the others, except in the immediate vicinity of the blockage, is very satisfactory.

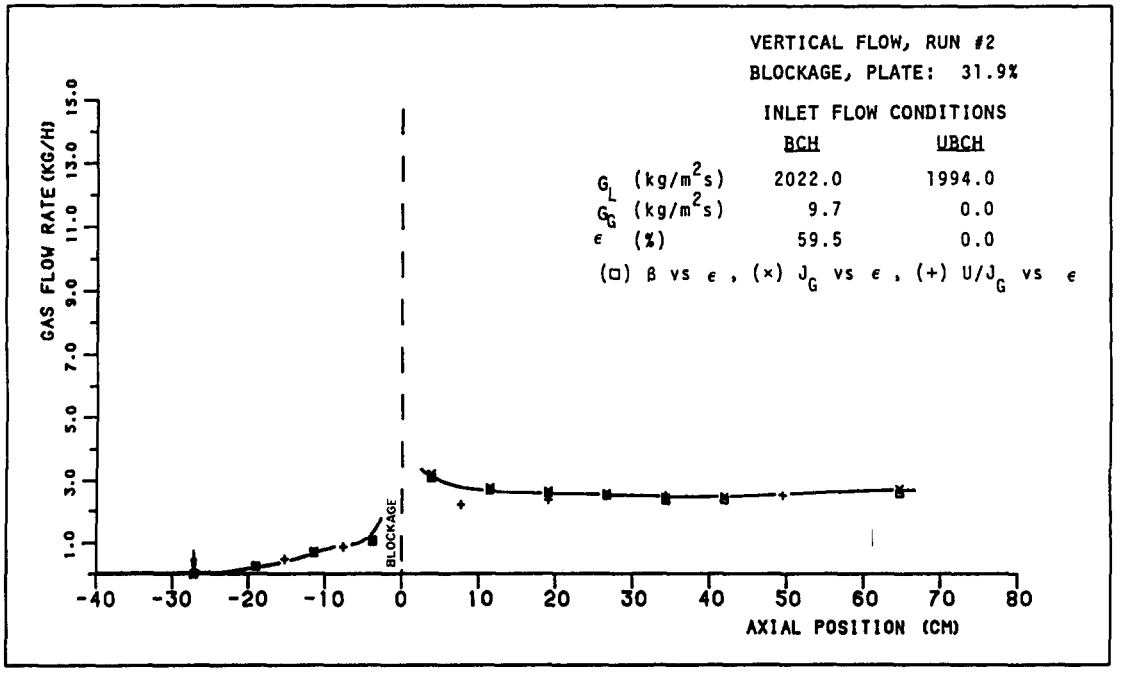

Figure 7.4b. Gas mass flow rates in the unblocked channel.

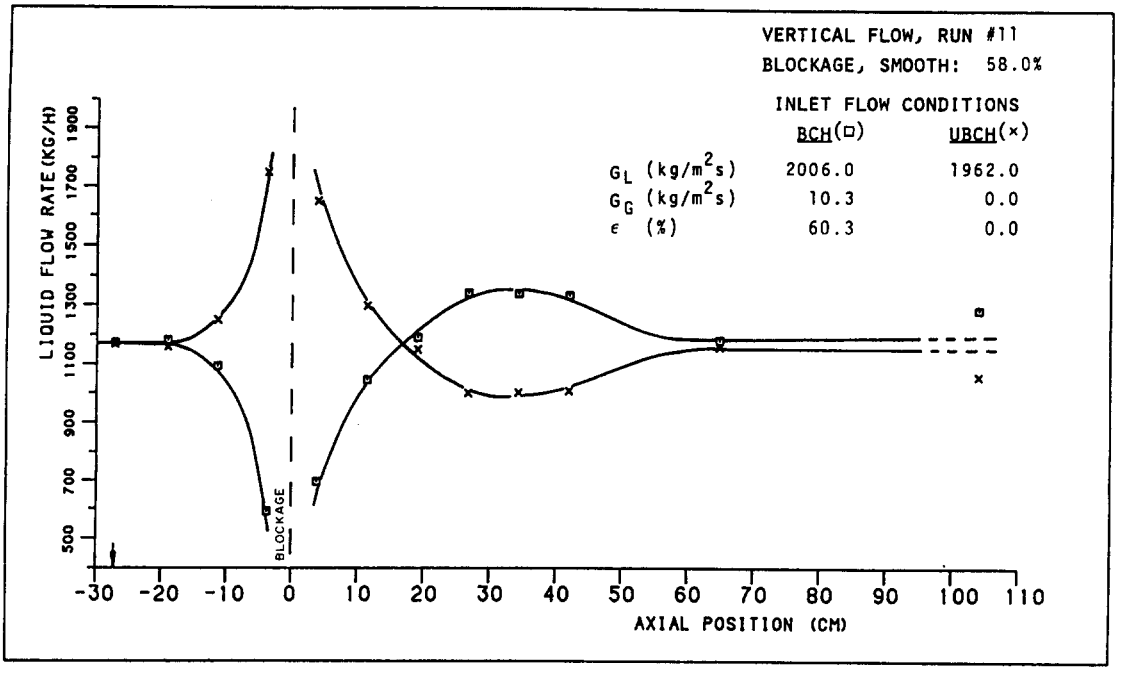

Figure 7.5a. Liquid mass flow rates in the blocked (BCH) and unblocked (UBCH) channels.

1. Equal void fractions at the inlet of the blocked and unblocked channels

The effect of the blockage on the gas mass transfer is felt as far as 120 mm (10 D_h) in the upstream region for all blockages (figures 7.1b, 7.2b and 7.3b) and the gas flow rate in the unblocked channel increases rapidly.

In the downstream region, gas flow rates in the unblocked channel for 30% plate (figure 7.1b) and 58% smooth blockage (figure 7.2b) first decrease and then increase. The minimum value observed during this variation was less than or equal to the flow rate at the inlet of the channel. Far from the blockage the flow rates return almost to their inlet values. For a 90% plate blockage (figure 7.3b), in the downstream region, the gas flow rate decreases very rapidly in the immediate

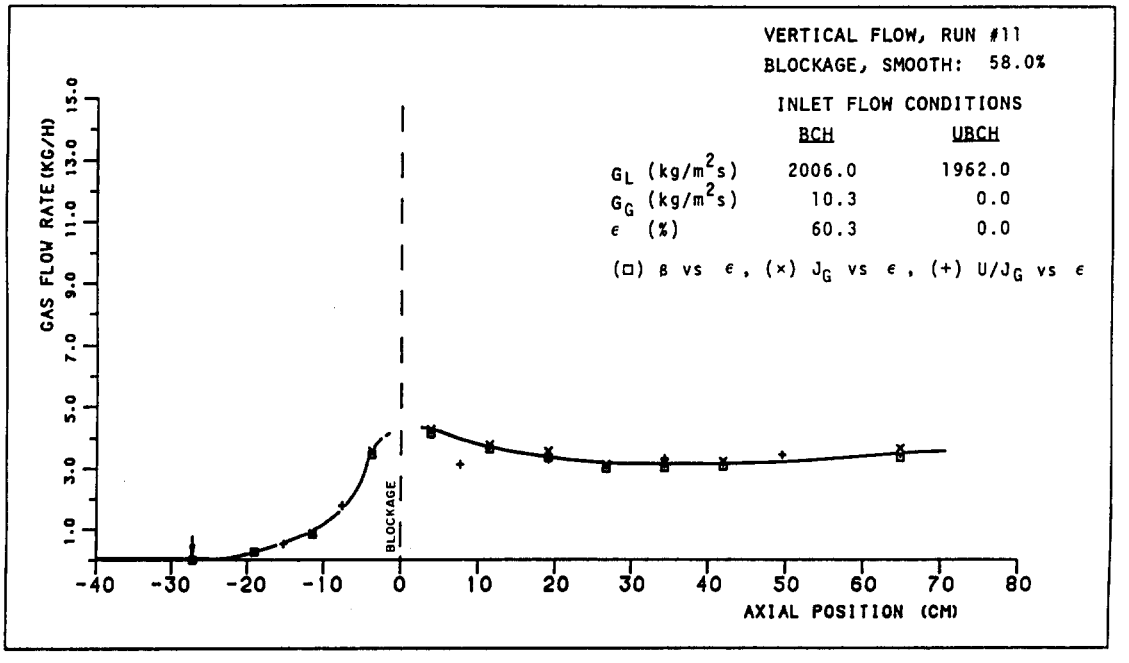

Figure 7.5b. Gas mass flow rates in the unblocked channel.

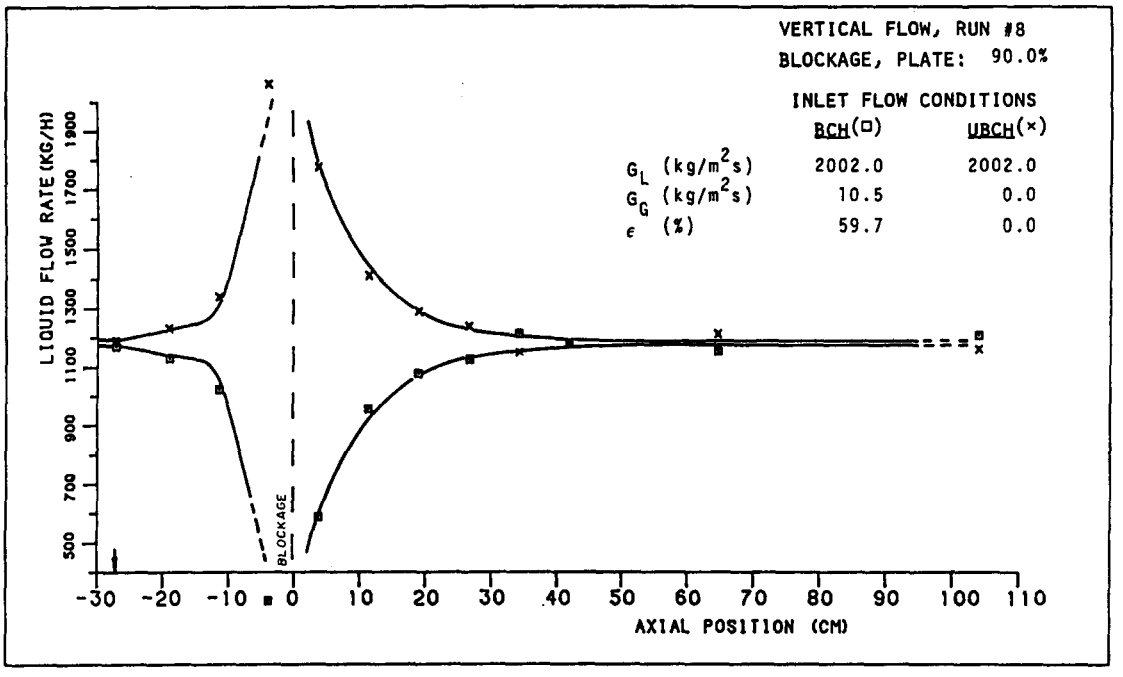

Figure 7.6a. Liquid mass flow rates in the blocked (BCH) and unblocked (UBCH) channels.

vicinity of the blockage and at a much slower rate in the outlying region. However, the flow rate in this region remains higher than that at the inlet of the unblocked channel.

2. Unequal void fractions with high void fraction at the inlet of the blocked channel

In the upstream region, because of the void migration caused mainly by pressure differences and void gradients between the channels, the gas transfer from the blocked channel to the unblocked channel starts with the beginning of the interconnected region (figures 7.4b, 7.5b and 7.6b). Figure 7.10b (Tapucu & Gençay 1980) shows the variation of gas flow rates in the low void channel of two laterally interconnected channels without blockage. Substantial gas

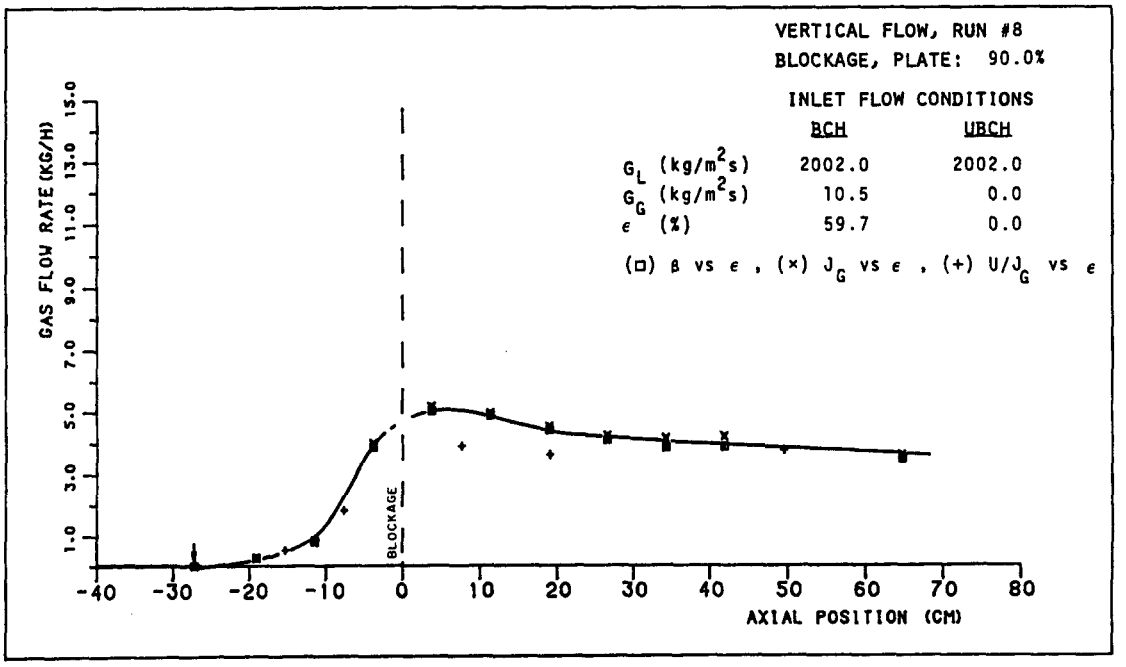

Figure 7.6b. Gas mass flow rates in the unblocked channel.

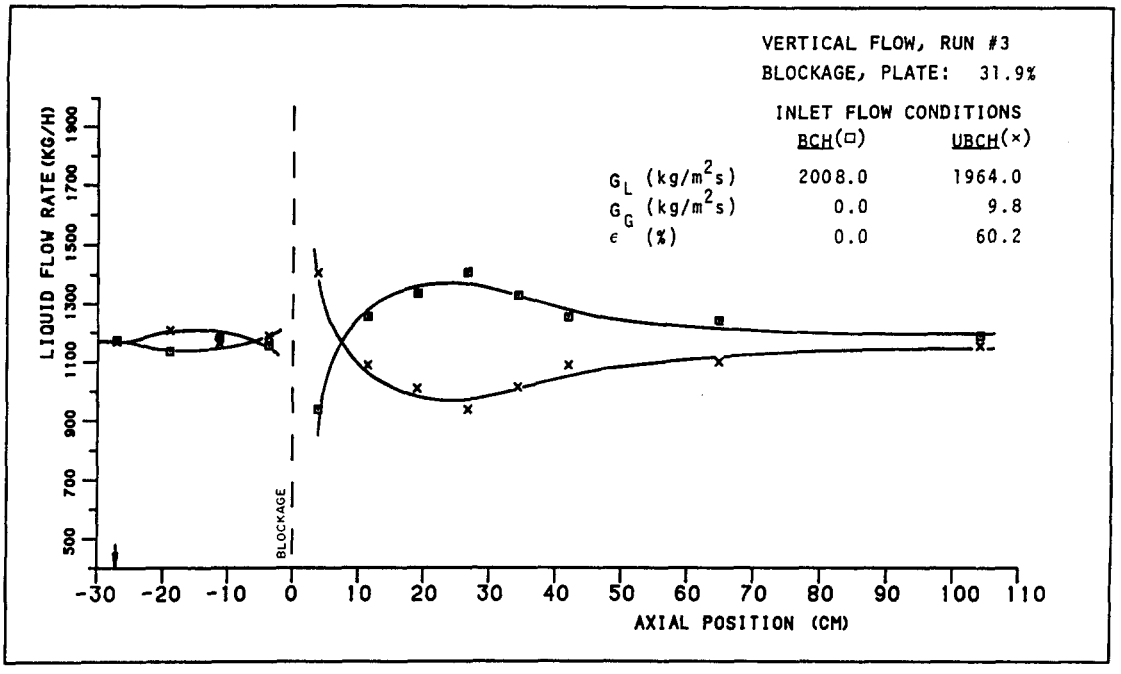

Figure 7.7a. Liquid mass flow rates in the blocked (BCH) and unblocked (UBCH) channels.

transfer has been observed from the high void channel to the low void channel. This transfer is the consequence of void migration from the high void channel to the low void channel. Far from the beginning of the interconnection, the void migration decreases appreciably as does the gas transfer. The same behavior has also been observed in the far upstream region of the blockage and, consequently, the gas flow rate in the unblocked channel starts increasing; when the effect of the blockage is felt, for example in figure 7.6b, the increase in flow rates becomes very substantial. In the downstream region, the unblocked channel retains most of the gas it has gained. Far from the blockage, the gas flow rates are either constant (figure 7.2b) or vary slightly (figures 7.5b and 7.6b).

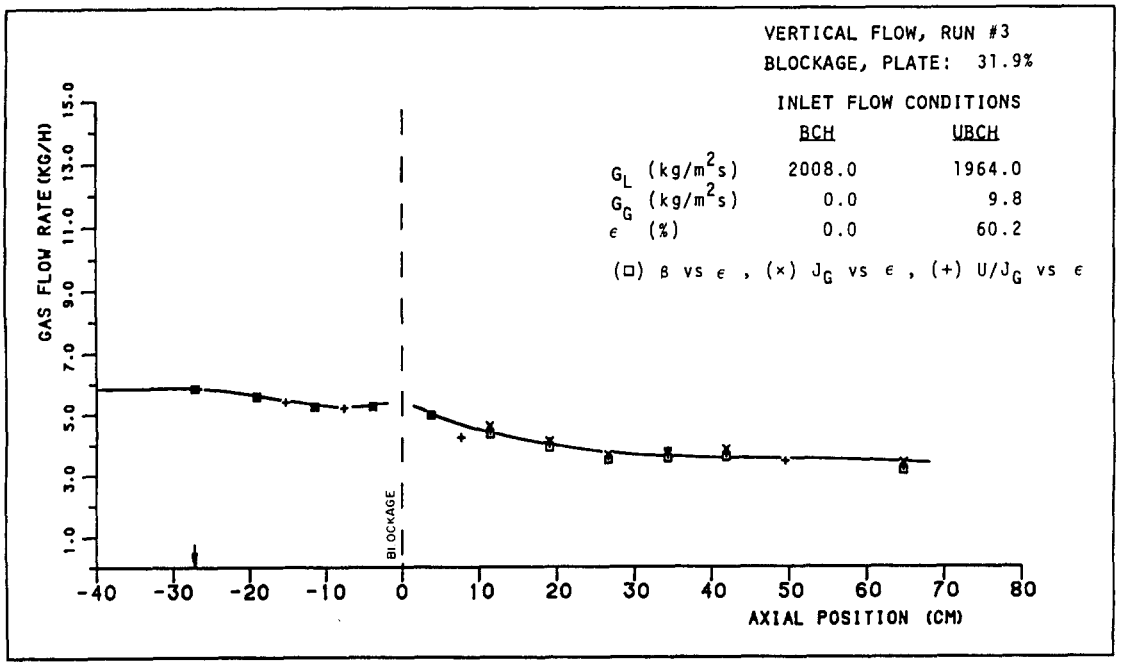

Figure 7.7b. Gas mass flow rates in the unblocked channel.

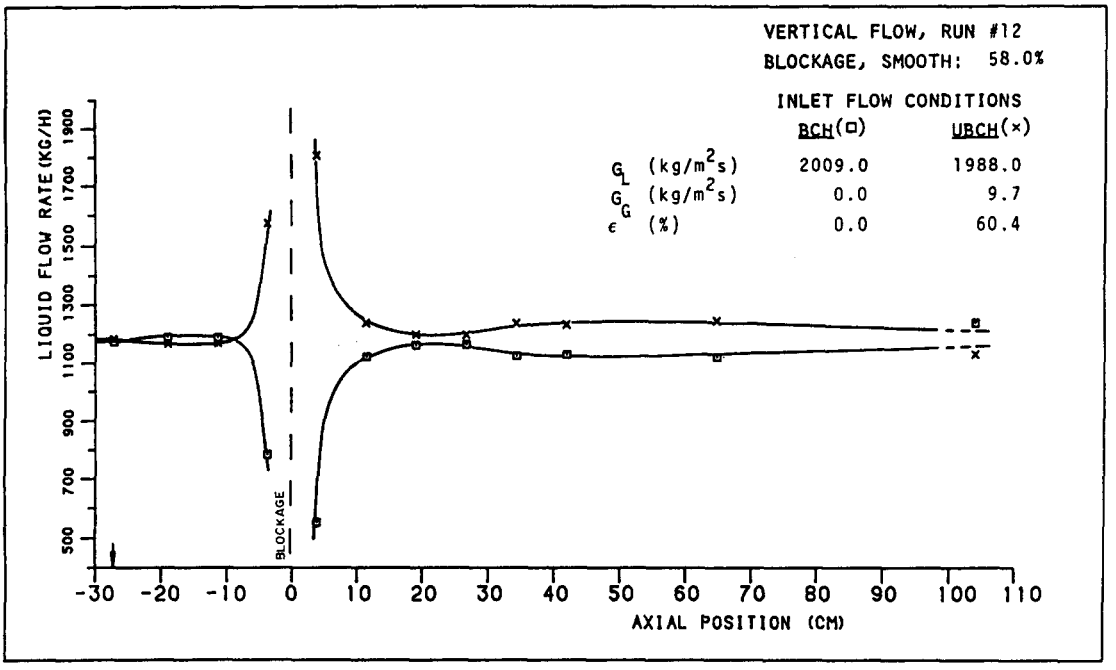

Figure 7.8a. Liquid mass flow rates in the blocked (BCH) and unblocked (UBCH) channels.

3. Unequal void fractions with high void fraction at the inlet of the unblocked channel

Because of the void migration, the gas flow rate in the unblocked channel starts decreasing at the beginning of the interconnections. Subsequently, this channel recovers some of the gas it has lost when the effect of the blockage is felt (approx. 120 mm upstream of the blockage, figures 7.7b, 7.8b and 7.9b). In the downstream region the flow rates decrease quite steadily to reach an asymptotic value.

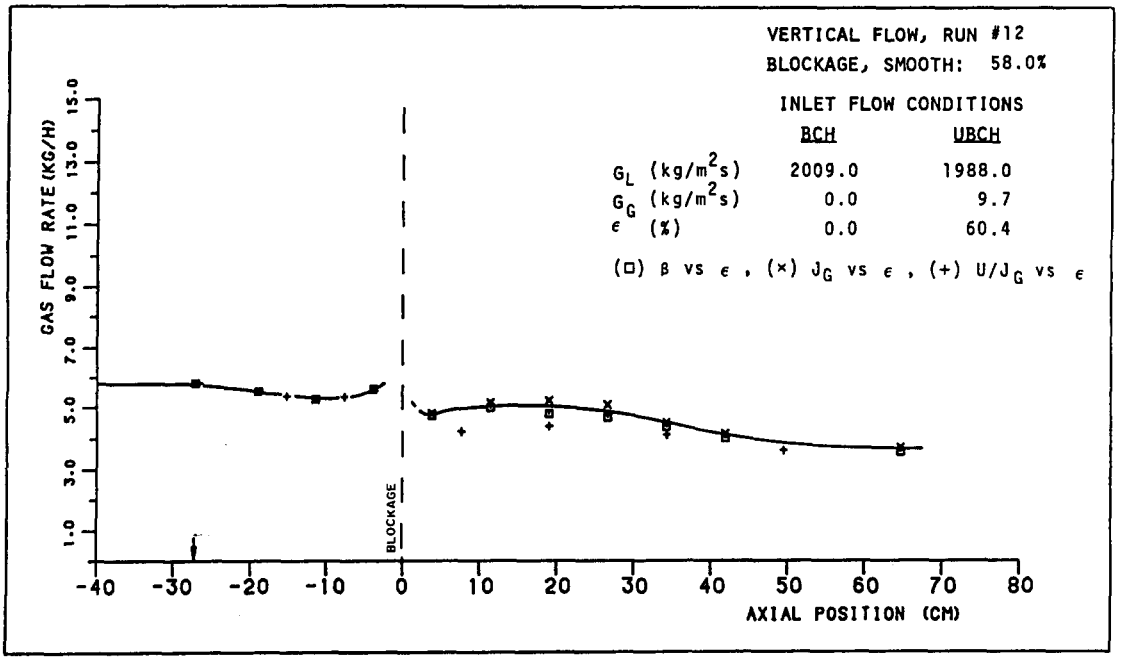

Figure 7.8b. Gas mass flow rates in the unblocked channel.

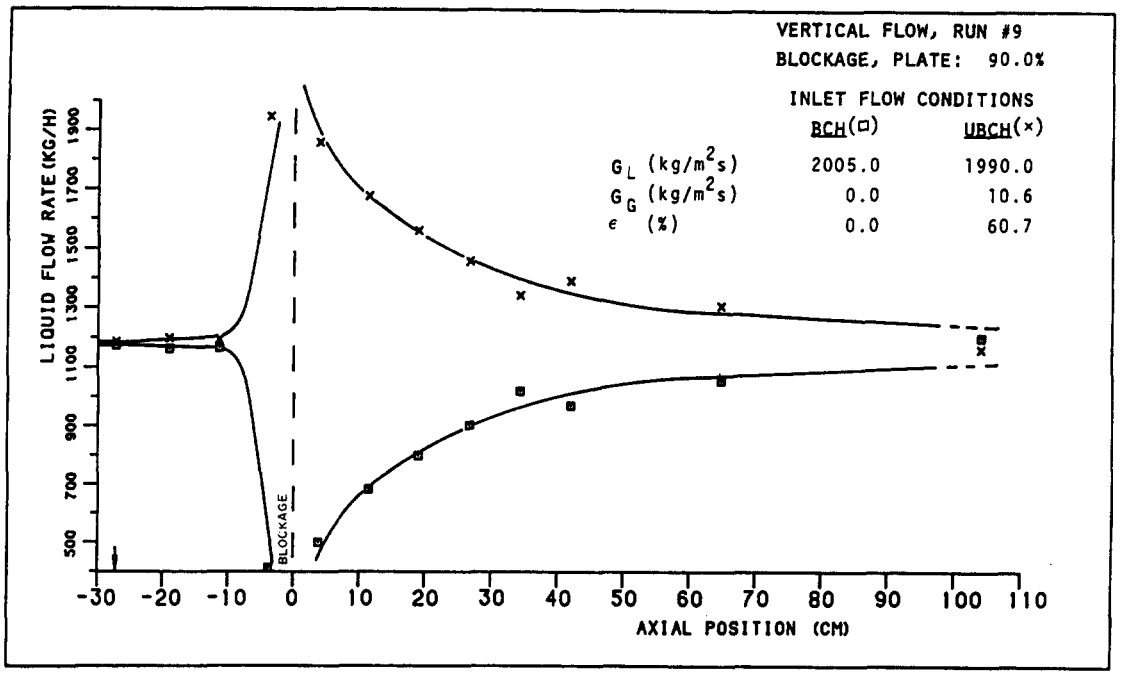

Figure 7.9a. Liquid mass flow rates in the blocked (BCH) and unblocked (UBCH) channels.

6. CONCLUSIONS

In this paper the axial distributions of liquid and gas mass flow rates in two laterally interconnected channels with blockages in one of them have been presented. The experiments were conducted on adiabatic two-phase flow which consisted of a mixture of air and water at 20°C. Two blockage configurations have been studied: plate and smooth. The shape of the latter was a cosine.

In the upstream region, the liquid mass transfer from the blocked channel to the unblocked channel is very important and increases with increasing blockage severity. For unequal voids at

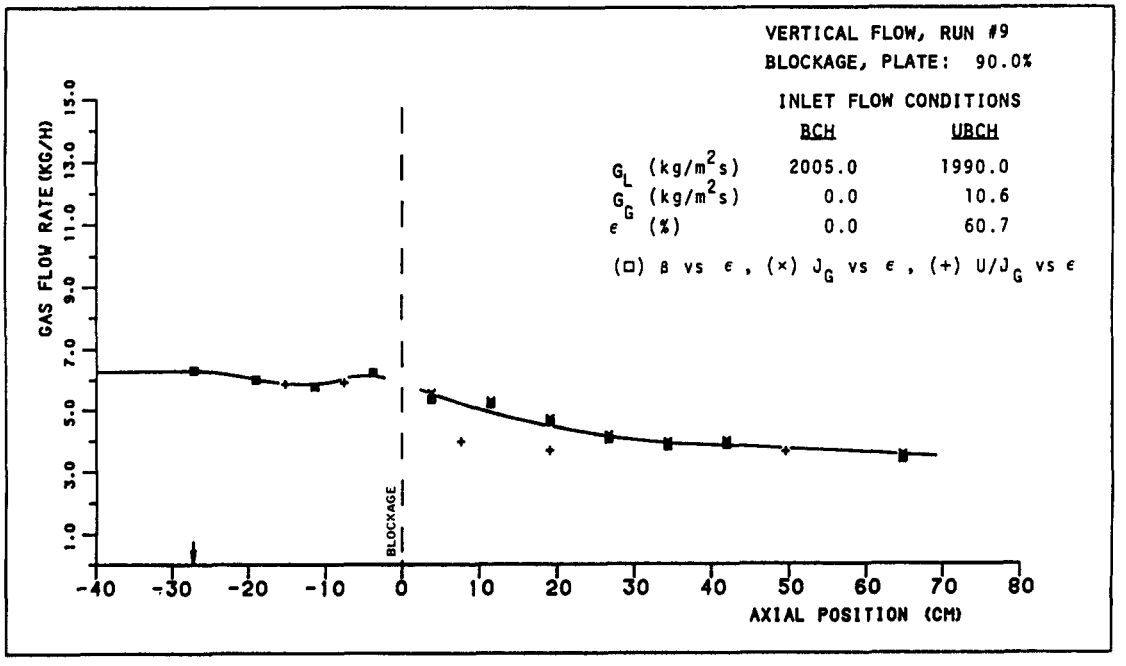

Figure 7.9b. Gas mass flow rates in the unblocked channel.

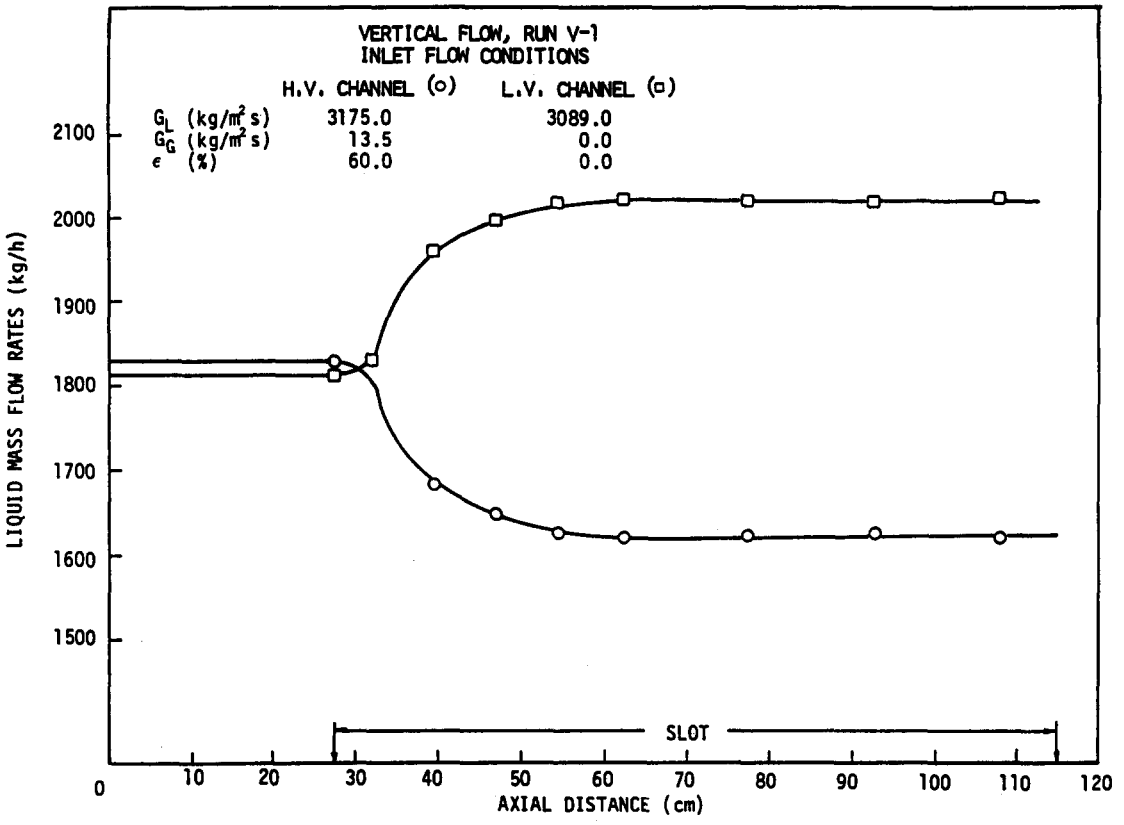

Figure 7.10a. Liquid mass flow rates in two laterally interconnected channels without blockage (Tapucu & Gençay 1980).

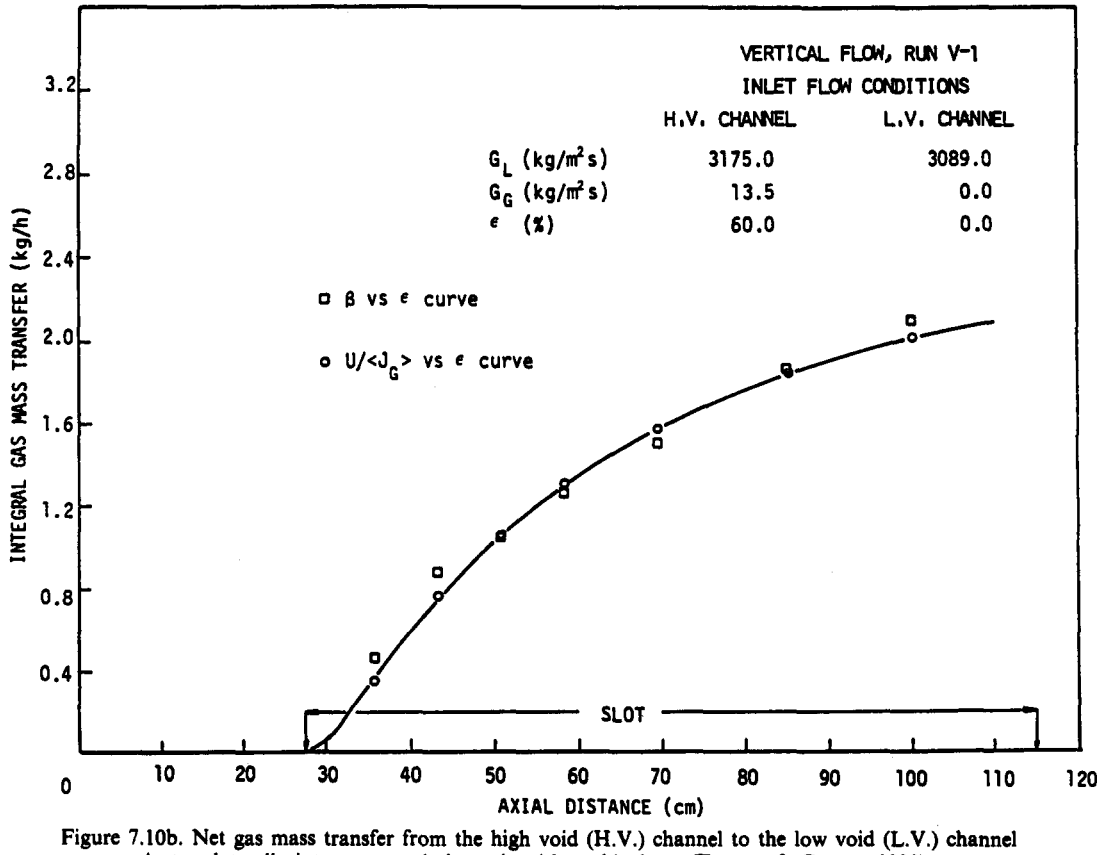

Figure 7.10b. Net gas mass transfer from the high void (H.V.) channel to the low void (L.V.) channel in two laterally interconnected channels without blockage (Tapucu & Gençay 1980).

the inlet of the channels, the liquid mass transfer immediately downstream of the beginning of the interconnection is mainly due to the entrainment effect of the bubbles during their migration from the high void channel to the low void channel and to the diversion cross-flow induced by the pressure differences between the channels. Therefore, depending on the channel in which the high void is introduced, the liquid mass transfer may take place from blocked channel to unblocked channel or vice versa. When the effect of the blockage is felt the transfer is always from blocked channel to unblocked channel mainly due to diversion cross-flow.

In the downstream region, the liquid mass exchanges between the channels are usually quite complex. Two general trends have been observed:

(i) The blocked channel first recovers more liquid than it lost. Consequently, the flow rates in this channel increase, go through a maximum and then decrease to an asymptotic value.
(ii) The blocked channel gradually recovers the liquid it has lost.

Two mechanisms are mainly responsible for the gas mass exchanges between the channels: diversion cross-flow where the driving force is the pressure difference between the channels, and turbulent void diffusion where the driving force is the void gradient between the channels. Void drift starts playing a role only far downstream of the blockage.

For equal void fractions at the inlet of the channels, the gas mass transfer from the blocked to unblocked channel occurs within a distance of 10 D_h upstream from the blockage. For unequal void fractions at the inlet of the channels, the gas mass transfer observed with the beginning of the interconnected region is the consequence of void migration (consisting mainly of diversion cross-flow and void diffusion) from the high void channel to the low void channel. Depending on the channel in which the void is introduced, the effect of the blockage is felt by a rapid increase in the gas flow rates in the unblocked channel (high void in the blocked channel) or by a decrease in the gas flow rate in the blocked channel when diversion cross-flow caused by the blockage overwhelms turbulent void diffusion (high void in the unblocked channel). In the region downstream of the blockage two kinds of behavior have been observed:

(a) the gas flow rate first decreases, goes through a minimum and then increases to an asymptotic value

or

(b) it decreases to an asymptotic value.

Acknowledgements—We are grateful to Mr P. Champagne and Mr J. C. Juneau for their technical constributions. This work was funded by the Electric Power Research Institute, Calif., U.S.A.

REFERENCES

BESTENBREUR, T. P. & SPIGT, C. L., 1970 Study on mixing between adjacent channels in an atmospheric air–water system. Report WW-030-R103.

BOWRING, R. W. & LEVY, J., 1969 Freon 7–rod cluster subchannel mixing experiments. Report AEEW-R663, Atomic Energy Est., Winfrith, U.K.

CASTELLANA, F. S. & CASTERLINE, J. E. 1972 Subchannel flow and enthalpy distributions at the exit of a typical nuclear fuel core geometry. *Nucl. Engng Des.* **22,** 3–18.

CREER, J. M., BATES, J. M. M., SUTEY, A. M. & ROWE, D. S. 1979 Turbulent flow in a model fuel rod bundle containing partial flow blockages. *Nucl. Engng Des.* **52,** 15–33.

GALBRAITH, K. P. & KNUDSEN, J. G. 1971 Turbulent mixing between adjacent channels for single-phase flow in a simulated rod bundle. Presented at the *12th National Heat Transfer Conf.*, Tulsa, Okla.

GENÇAY, S., TAPUCU, A., TROCHE, N. & MERILO, M. 1984 Experimental study of the diversion cross-flow caused by subchannel blockages. Part I: experimental procedures and mass flow rates in the channels. *J. Fluids Engng* **106,** 435–440.

GONZALEZ-SANTALO, J. M. 1971 Two-phase flow mixing in rod bundle subchannels Ph.D. Thesis, MIT, Cambridge, Mass.

HETSRONI, G., LEON, J. & HAKIN, M. 1968 Cross-flow and mixing of water between semiopen channels. *Nucl. Sci. Engng* **34,** 189–193.

KHAN, E. U., KIM, K. & LINDSTROM, E. D. 1971 Cross-flow resistance and diversion cross-flow mixing between rod bundles. *Trans. Am. nucl. Soc.* **14,** 249–254.

KJELLSTRÖM, B. 1972 Transport process in turbulent channel flow. Report AE-RL-1344, AB Atomenergi, Sweden.

LAHEY, R. T. JR & SCHRAUB, F. A. 1969 Mixing, flow regimes and void fraction for two-phase flow in rod bundles. Presented at the *Symp. on Two-phase Flow Heat Transfer in Rod Bundles; ASME Winter A. Heat Transfer Mtg*, Los Angeles, Calif.

LAHEY, R. T. JR, SHIRALKAR, B. S. & RADCLIFFE, D. W. 1971 Mass flux and enthalpy distribution in a rod bundle for single and two phase flow conditions. *Trans. ASME Jl Heat Transfer* **93,** 197–209.

LAHEY, R. T. JR, SHIRALKAR, B. S., RADCLIFFE, D. W. & POLOMIK, E. E. 1972 Out-of-pile subchannel measurements in a nine-rod bundle for water at 1000 psia. In *Progress in Heat and Mass Transfer*, Vol. VI. Pergamon Press, New York.

LYALL, H. G. 1971 Measurement of flow distribution and secondary flow in ducts composed of two square interconnected subchannels. Presented at the *Symp. on Internal Flows*, Salford, U.K.

NIKURADSE, J. 1926 Untersuchungen über die Geschwindgkeitsverteilung in turbulenten Strömungen. Thesis, Göttingen. *VDI Forsch. Hft 281.*

PETRUNIK, K. 1973 Turbulent interchange in simulated rod bundle geometries for genetron-12 flows. Ph.D. Thesis, Univ. of Windsor, Ontario.

PRANDTL, L. 1926 Über den Reibungswiderstand strömenderLuft. *Ergebn. aerodyn. VersAnst. Göttingen Ser. III.*

ROGERS, J. T. & TAHIR, A. E. E., 1975 Turbulent interchange mixing rod bundles and the role of secondary flows. ASME Paper 75-HT-31.

ROGERS, J. T. & TODREAS, N. E. 1968 Coolant interchannel mixing in reactor fuel rod bundle–single phase coolants. Presented at the *Symp. on Heat Transfer in Rod Bundles; ASME Winter A. Heat Transfer Mtg*, New York.

ROUSEL, A. & BEGHIN, A. 1966 Etude de la répartition des débits dans une section d'essais à deux canaux. Papport Euratom No. 25.

ROWE, D. S. & ANGLE, C. W. 1967 Experimental study of mixing between rod-bundle fuel-element flow channels during boiling—Part II. Measurement of flow and enthalpy in two parallel channels. Report BNWL-371, Part 2.

ROWE, D. S. & ANGLE, C. W., 1969 Cross flow mixing between parallel flow channels during boiling—Part III. Report BNWL-371, Part 3.

ROWE, D. S., WHEELER, C. L. & FITZSIMMONS, D. E. 1973 An experimental study of flow and pressure in rod bundle subchannels containing blockages. Report BNWL-1771.

RUDZINSKI, K. F., KULDIP, S. & ST PIERRE, C. C. 1972 Turbulent mixing for air–water flows in simulated rod bundle geometries. *Can. J. chem. Engng* **50,** 297–299.

SHOUKRI, M., TAWFIK, H. & MIDIVI, W. I. 1982 An experimental investigation of two-phase flow interactions in horizontal rod bundle geometries. In *Proc. 7th Int. Heat Transfer Conf.*, Munich, pp. 355–360.

SINGH, K. 1972 Air–water turbulent mixing in simulated rod bundle geometries. Ph.D. Thesis, Univ. of Windsor, Ontario.

SKINNER, V. R., FREMAN, A. R. & LYALL, H. G. 1969 Gas mixing in rod clusters. *Int. J. Heat Mass Transfer* **12,** 265–278.

STIEFEL, V. 1971 Comparison of measured and calculated mass flow distribution in partially blocked flow channels. EIR Report TM-IN-408.

TAHIR, A. & CARVER, M. B. 1984 Comparison of ASSERT subchannel code with Marviken bundle data. Report AECL-8352.

TAPUCU, A. 1977 Studies on diversion cross-flow between two parallel channels communicating by a lateral slot. I: transverse flow resistance coefficient. *Nucl. Engng Des.* **42,** 297–306.

TAPUCU, A. & GENÇAY, S. 1980 Experimental investigation of mass exchanges between two laterally interconnected two-phase flows, Part 1. Report CDT-P-533, École Polytechnique de Montréal, Québec.

TAPUCU, A., GENÇAY, S., TROCHE, N. & MERILO, M. 1984a Experimental study of the diversion cross-flow caused by subchannel blockages. Part II: pressures in the channels and the comparison of COBRA III-C predictions with experimental data. *J. Fluids Engng* **106,** 441–447.

TAPUCU, A., GENÇAY, S. & TROCHE, N. 1984b Experimental study of diversion cross-flow caused by subchannel blockages. Single-phase flow. Report NP-3459, Vol. 1, EPRI, Palo Alto, Calif.

TAPUCU, A., GIRARD, R., TEYSSEDOU, A. & TROCHE, N. 1986 Experimental investigation of void migration between two laterally interconnected two-phase flows (void profiles and effect of liquid mass flux). Report CDT-P-1021, École Polytechnique de Montréal, Québec.

TAPUCU, A., TEYSSEDOU, A., GEÇKINLI, M. & TROCHE, N. 1988 Experimental study of the diversion cross-flow caused by subchannel blockages. Part II: two-phase flow. Report NP-3459, Vol. 2, EPRI, Palo Alto, Calif.

TRUPP, A. C. & AZAD, R. S. 1975 The structure of turbulent flow in triangular array rod bundles. *Nucl. Engng Des.* **32,** 47–84.

VAN DER ROS, T. 1970 On two-phase flow exchange between interacting hydraulic channels. Doctorate Thesis, Eindhoven Univ. of Technology, The Netherlands.

WALTON, F. B. 1969 Turbulent mixing measurements for single-phase air, single-phase water and two-phase air–water flows in adjacent triangular subchannels. M.A.Sc. Thesis, Univ. of Windsor, Ontario.

WEISMAN, J. 1971 Cross-flow resistance in rod-bundle cores. *Nucl. Technol.* **15,** 465–468.